Observations of Lick standard stars using the SCORPIO multi-slit unit at the SAO 6-m Telescope

Sharina M.E.[1*], Afanasiev V.L.[1], Puzia T.H.[2]

[1] *Special Astrophysical observatory Russian Academy of Sciences, N.Arkhyz, KChR, 369167, Russia*

[2] *Space Science Telescope Institute, 3700 Sun Martin Drive, Baltimore, MD21218, USA*

Abstract

We present Lick line-index measurements of standard stars from the list of Worthey (1994). The spectra were taken with the multi-slit unit of the SCORPIO spectrograph at the 6-m Special Astrophysical observatory telescope. We describe in detail our method of analysis and explain the importance of using the Lick index system for studying extragalactic globular clusters. Our results show that the calibration of our instrumental system to the standard Lick system can be performed with high confidence.

Key words: methods of data reduction, line strength, abundance

———————————————

*e-mail: sme@sao.ru

Introduction

Studying the line-strength indices plays an important role in analysing the ages, metallicities, and [α/Fe] ratios of unresolved distant stellar populations. The behavior of indices in composite stellar systems has supplied fundamental clues to the understanding the star formation histories of galaxies (e.g. Faber 1973, Burstein et al. 1984).

Globular clusters (GCs) are simple stellar systems composed of stars of one age and chemical composition and offer a unique tool to access the star formation histories of their own galaxies. GCs are gravitationally bound objects, whose lifetimes may exceed the Hubble time. They are the most luminous simple stellar populations known to exist. If the correlations between key spectral indices, metallicities and ages are common for GCs in all types of galaxies, we can determine the age for the given particular GC by comparison with evolutionary population synthesis models (e.g. Worthey 1994, Vazdekis 1999, Bruzual & Charlot 2003, Thomas et al. 2003).

We observe GCs in nearby galaxies using the multi-slit unit of the SCORPIO spectrograph, mounted at the prime focus of the 6m telescope. Our ultimate objective is to study the star formation and chemical enrichment histories of globular cluster systems and their host galaxies. However, first, we will check the correspondence of our instrumental system of line-strength indices to the Lick standard system. In the following we study the influence of random and systematical errors arising in the process of observation and data reduction on the Lick index measurements.

Spectrophotometric system of Lick indices.

Definitions

Understanding the physical origin of prominent absorption features in the integrated light of simple and composite stellar systems (i.e. star clusters and galaxies) is based on an empirical study of variations of these features in Galactic stars with effective temperature, mass, and chemical composition. For this, Worthey et al.

(1994) measured indices for a sample of 460 Galactic stars. Spectra in a range of 4000–6000 Å were obtained in the Lick observatory in 1972-1984 using the same instrumentation. Spectral resolution of the Lick system is 8–10 Å (Worthey & Ottaviani 1997). Information about the measured indices for stars with various $logg$, T_{eff} and $[Fe/H]$ is used to construct the fitting functions, which are the main ingredients for computing theoretical models of simple stellar populations.

Despite the existence of different approaches to measuring the line-strength indices, most of the authors adhere to the classical definition of the indices as an analog of the equivalent width (e.g. Faber 1973, Puzia et al. 2002):

$$W_\lambda = \int_{\lambda_{min}}^{\lambda_{max}} \left(1 - \frac{F_l(\lambda)}{F_c(\lambda)}\right) d\lambda, \tag{1}$$

where $F_l(\lambda)$ is the observed spectrum and $F_c(\lambda)$ is the local continuum, which is usually determined via interpolating $F_l(\lambda)$ between two neighbouring spectral ranges on the red and blue sides of the line.

The so-called theoretical way of the index calculation

$$I_t(\lambda) = \left(1 - \frac{\int F_l(\lambda)d\lambda}{\int F_c(\lambda)d\lambda}\right) \cdot \Delta\lambda, \tag{2}$$

does not differ strongly from the "observational" definition (1) for spectra with a high S/N ratio. There are no systematic differences between the two definitions. The scatter is $< 0.1\%$. $I_t(\lambda)$ is the most common definition and yields more plausible results for spectra with low S/N (≤ 10 per Å). The observational definition is commonly used in the literature.

In order to avoid subjectivity in drawing the local continuum, the line-strength indices are completely characterized by three wavelength ranges: one central one, which includes the spectroscopic feature, and two neighbouring ones located towards the red and blue of the central region (http://astro.wsu.edu/worthey/html/index.table.html). Geisler (1984) and Rich (1988) pointed out that a pseudo-continuum is measured instead of true continuum at low spectral resolution. Molecular line-strength indices are usually measured in magnitudes:

$$I_m(mag) = -2.5 \cdot \log_{10}\left(1 - \frac{W_\lambda(\text{Å})}{\Delta\lambda}\right),$$

where $\Delta\lambda$ is the width of the central wavelength range. Molecular indices are commonly used to measure broad molecular features in spectra. The continuum regions for them are located far from the central region.

Atomic indices are measured in Ångstroms:

$$I_a(\text{Å}) = \Delta\lambda(1 - 10^{-0.4\,I_m}).$$

In that case, the lines and the central wavelength regions have narrower width. The continuum regions are closer to the central bandpasses.

Error estimation in the measurement of the Lick indices

Obviously, the suitability of line-strength indices to investigate the above mentioned items relies on the proper determination of the associated index errors.

There are the following sources of systematic errors in the line-index measurements: flux calibration uncertainties, corrections from spectral resolution and velocity dispersion, sky subtraction uncertainties, scatter light effects, wavelength calibration and radial velocity errors, seeing and focus length variations, deviations from linearity, and contributions from nebular emission lines. The statistical errors arise from the random Poissonian noise.

Observations and data reduction

Instrumental characteristics

The observations were performed with the multi-slit unit of the SCORPIO spectrograph (Afanasiev & Moiseev 2005). In this mode SCORPIO has 16 movable slits (1.2" x 18") in the field of 2.9 x 5.9 arcminutes in the focal plane of the telescope. We use the CCD detector EEV42-40 with 2048 x 2048 pixel elements and the scale ~ 0.18 arcminutes per pixel. The holographic grism VPHG1200g (1200 lines/mm) gives a spectral resolution ~ 5 Å. The exact covered spectral region depends on the distance from the center of the field. Most of the spectra have good wavelength coverage between 4000–6000 Å.

The original, non-reduced spectra obtained with SCORPIO in multi-slit mode are shown in Fig. 1.

A log of observations of Lick standard strar is given in Table 1. Resulting spectra of ten standard stars are shown in Fig. 2.
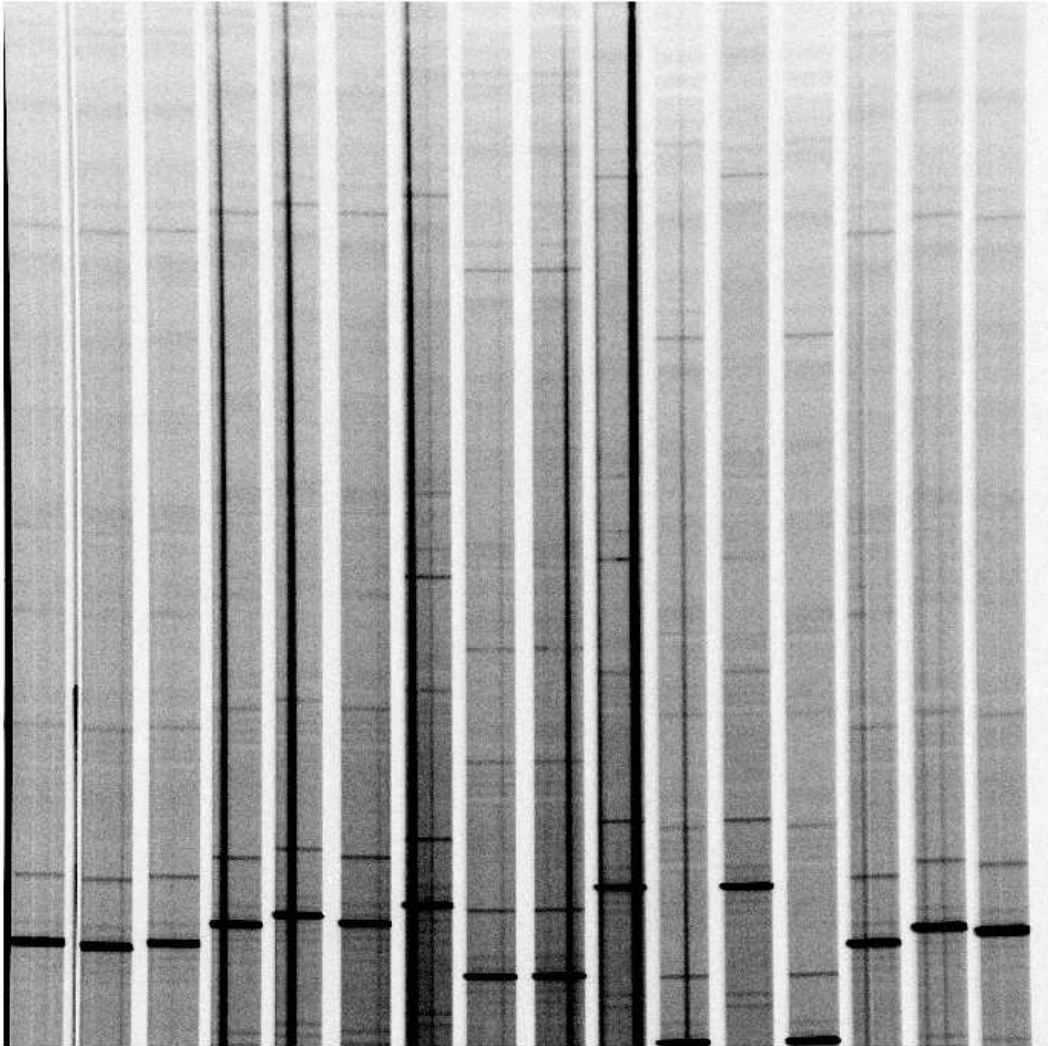
Figure 1: Initial, non-reduced image obtained with SCORPIO in multi-slit mode.

Data reduction

The data reduction was carried out using software packages written in the Inter-active Data Language (IDL). First, we performed the standard primary reduction of our spectra: bias subtraction, cosmic particles removal, and bad pixel replacement.

To properly determine the edges of our spectra for their subsequent extraction, we remove the traces of bright light near slits 15 and 16 (see Fig. 1) from the image. This cosmetic procedure was carried out on flat-field images. The result of the subsequent determination of the edges of our 16 spectra was applied to all spectra:

Table 1: Observational log

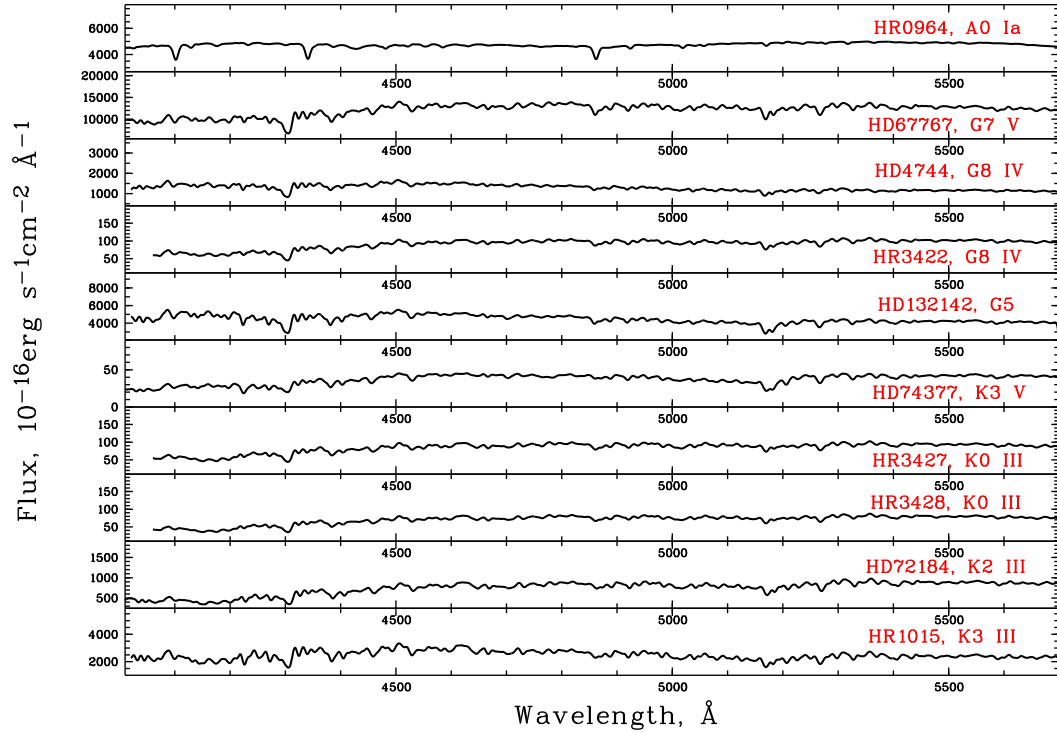| Object	Date	Exposure	Seeing
HD132142	15.09.2004	10 c.	1"
HD4744	15.09.2004	30 c.	1"
HR1015	15.09.2004	10 c.	1"
HD67767	16.12.2004	120 c.	3"
HD72184	16.12.2004	20x2, 40 c.	3"
HD74377	15.12.2004	120, 240 c.	3"
HR0964	16.12.2004	20, 40 c.	3"
HR3422	15.12.2004	120x2 c.	3"
HR3427	15.12.2004	120x2 c.	3"
HR3428	15.12.2004	120x2 c.	3"

Figure 2: Flux calibrated spectra of the Lick standard stars.

the reference spectra and the spectra of standard stars; and should be applied to to all our globular cluster spectra.

Correcting the geometric field distortions on the reduced spectra in X and Y directions (see Fig. 1) is the most important data reduction step. We compute a polynomial of transformation between the final uniform grid corresponding to the edges of spectra and the initial distorted one. The grid is drawn with a uniform step along Y coordinate. The edges of the spectra serve as the reference points for straightening the spectra. To find these edges, we divide the original distorted image into 10-pixel-long areas along the Y coordinate. These areas are summed in one-dimensional spectra for which the intensity maxima are sought. The derived coordinates of the maxima are the edges of the spectra. The IDL POLY2D procedure is used to find the polynomial transformation between two images represented by the corresponding reference points and to calculate the succeeding transformation to the rectified image. The image is corrected according to a polynomial of the form:

$$x' = a(x, y) = \sum_{i=0}^{N} \sum_{j=0}^{N} P_{i,j} x^j y^i$$

$$y' = b(x, y) = \sum_{i=0}^{N} \sum_{j=0}^{N} Q_{i,j} x^j y^i,$$

where tensors P and Q contain polynomial coefficients. Each 2x2 tensor contains $(N + 1)^2$ elements. We apply this transformation formulae to all the multi-slit spectra.

After the correction for the field distortion, we identify lines in the spectrum of a reference He-Ne-Ar lamp, calculate dispersion curves, and perform linearization in wavelength space.

Since the instrumental conditions and the data reduction steps are identical for the flat fields the spectra of the objects, we have the right to divide the object frames by the flat field after the linearization of the spectra, not after bias subtraction and cosmic particle hits removal, as is usually done. The multislit spectrum reduction procedure is complex, because of the distortion of spectra in the focal plane needs to be corrected.

Subsequently, the sky spectrum is subtracted. Using a the least-square method, the sky spectrum is interpolated in the spatial direction and subtracted from the object spectrum. Unfortunately, the sky subtraction method cannot be applied
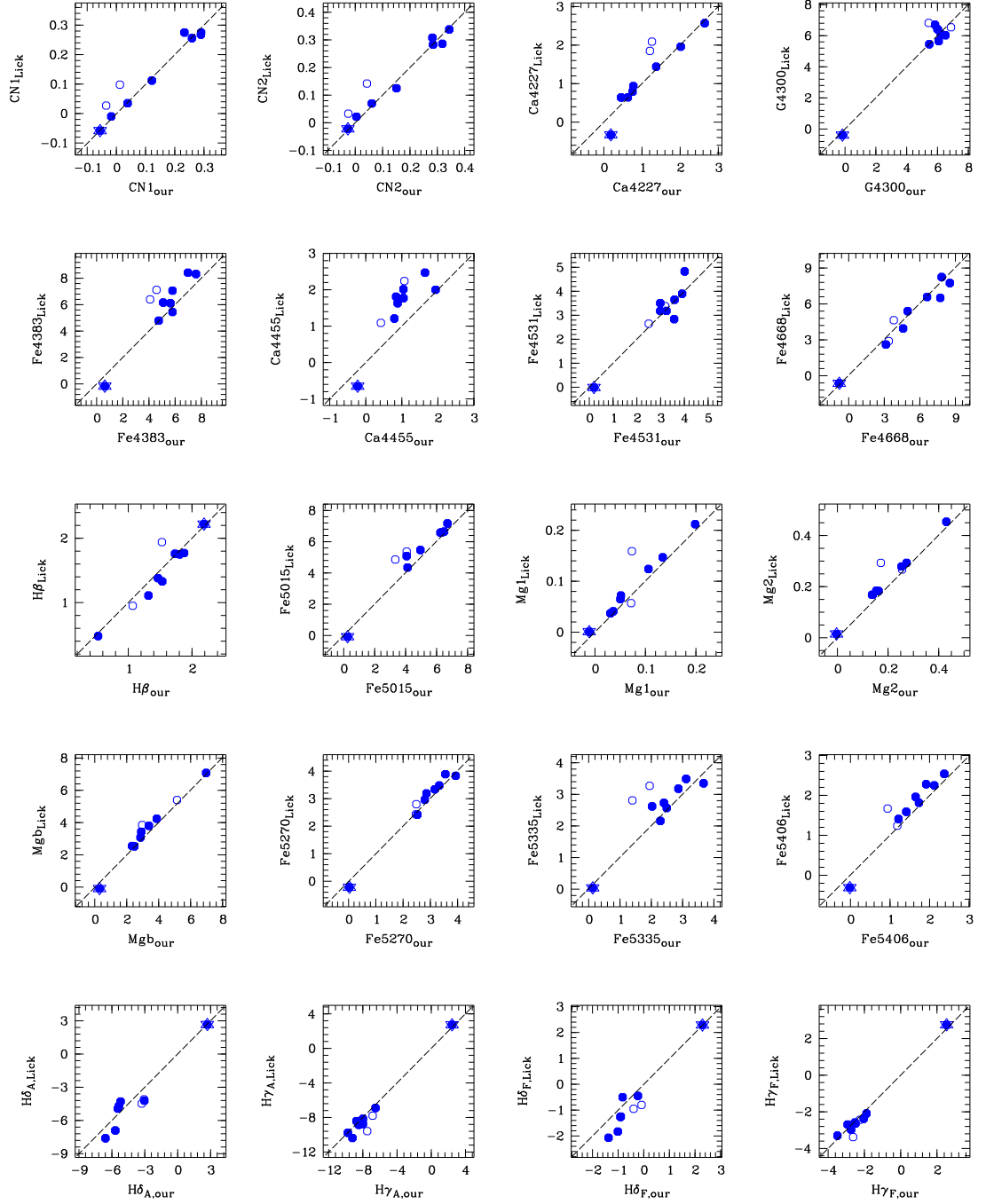
Figure 3: Comparison of passband measurements of our spectra and original Lick data for 10 Lick standard stars. The dashed line shows the one-to-one relation. Two outliers (HD132142 and HD4744) are shown as open circles and were excluded from calculations of the Lick transformation. The early A-type supergiant HR0964 (a star-like symbol) shows strongly negative Ca4227, Ca4455 and Fe5406 index values in the calatog of Worthey et al. (1994), and the lowest statistical weight was assigned to it.

to bright Lick standard stars. Even on short exposures the light of a bright star floods the entire slit. However, in this case the sky background contributes only slightly to the final spectrum. Occasionally, we detected scattered light between the slits. In this case, it is more appropriate to subtract the sky spectrum taken from the other (spatially close, but not neighbouring) slits. In the next section we show that the Lick indices change only slightly (i.e. within the limits of the random measurement errors) after this procedure. A similar approach to the sky subtraction might be applied for the reduction of the integrated-light spectra of extragalactic GCs, although the expected flux from the object in this case will not flood the entire slit, giving rise to scattered light.

We use spectroscopic standard stars observed on the same night through the medium slit to calibrate the fluxes of all Lick standard star spectra. It should be noted that, by definition, the procedure of calculating the Lick indices does not require the absolute flux calibration (equations (1) and (2)). Hence, applying of the flux calibration to standard star and the object spectra significantly reduces the non-linear transformation offsets to the Lick system for indices with broad passband definitions, since these indices are sensitive to the rate of change in the continuum slope.

It is important to observe objects and standard stars in the same instrumental conditions to correctly calculate the Lick indices. In other words, the spectral sensitivity should be the same during our observations. Therefore, we obtain the spectra for globular clusters and standard stars using the same multi-slit mode.

Transformation from the SCORPIO to the Lick system

Before measuring the indices, we degraded our spectra to the resolution of the Lick system. The effective resolution (FWHM) of our spectra was determined as a full width at half maximum (FWHM) of the corresponding autocorrelation function divided by $\sqrt{2}$ (Tonry & Davis, 1979). Our resolution correction technique consisted of broadening our spectra to the Lick resolution with a Gaussian filter with the dispersion

$$\sigma_{smooth}(\lambda) = \left(\frac{\text{FWHM}(\lambda)^2_{Lick} - \text{FWHM}(\lambda)^2_{data}}{8 \ln 2} \right)^{1/2},$$

Table 2: Summary of the coefficients α and β and the rms errors of the linear transformation to the standard system for all index measurements. The fifth and sixth columns show units of the indices and mean bootstrapp errors of the index values for 10 standard stars. The last column shows a mean standard deviation of index values for the stars with the indices measured on 13 spectra obtained by subtracting the sky spectrum taken from different (not neighbouring) slits.

Index	α	β	rms	units	$\sigma(\text{Index})$	$\sigma(\text{Index})_{msl}$
CN1	0.036	-0.0085	0.015	mag	0.0022	0.0027
CN2	0.052	-0.143	0.041	mag	0.0040	0.0018
Ca4227	0.365	-0.008	0.185	Å	0.097	0.0123
G4300	0.786	-0.086	0.713	Å	0.105	0.0198
Fe4384	-0.202	0.362	1.661	Å	0.117	0.0250
Ca4455	0.650	-0.001	0.324	Å	0.120	0.0085
Fe4531	-0.068	0.186	0.324	Å	0.126	0.0160
Fe4668	0.223	-0.054	0.731	Å	0.141	0.0199
Hβ	-0.339	0.124	0.053	Å	0.141	0.0070
Fe5015	0.279	0.145	0.584	Å	0.148	0.0160
Mg$_1$	0.016	0.014	0.034	mag	0.0048	0.0002
Mg$_2$	0.018	0.007	0.011	mag	0.0048	0.0003
Mgb	0.064	0.054	0.271	Å	0.154	0.0067
Fe5270	-0.287	0.198	0.186	Å	0.157	0.0088
Fe5335	0.312	0.073	0.444	Å	0.157	0.0059
Fe5406	0.239	-0.018	0.150	Å	0.158	0.0051
Hδ_A	-0.647	0.035	1.340	Å	0.178	0.1600
Hγ_A	-0.056	0.083	0.901	Å	0.188	0.0344
Hδ_F	-0.348	-0.038	0.451	Å	0.194	0.0450
Hγ_F	-0.069	0.117	0.463	Å	0.196	0.0180

taking into account the wavelength-dependent resolution of the Lick system (see Worthey & Ottaviani 1997). Lick indices were measured on the spectra corrected for radial velocities. Figure 3 shows the comparison between the Lick data and our index measurements for all passbands. Least-square fits are used to parameterize

the deviations from the Lick system as a linear function of wavelength:

$$EW_{cal} = \alpha + (1 + \beta)EW_{raw},$$

where EW_{cal} and EW_{raw} are calibrated and raw indices, respectively. Table 2 summarizes the individual coefficients α and β. It is seen that our instrumental system satisfactorily reproduces the standard Lick system, in particular in the important indices such as Mgb, Mg$_2$, Fe5270, Fe5335, and all Balmer indices.

It is interesting to note, that $\sim$20% of atomic metal line indices have negative values for O, B, A spectral type stars in the catalog of Worthey et al. (1994). This is probably due to the high probability of chemical peculiarities for young hot stars (see spectroscopic atlases: e.g. Chentsov et al. 2003, Albayrak et al. 2003). Broad pseudocontinuum regions include many absorption line features that are much more intense than the studied ones. Thus, the flux per unit wavelength in the index passbands appear to be lower than the corresponding fluxes in the pseudocontinuum regions.

The influence of different sky subtraction methods on the Lick index measurements is illustrated in the last column of Table 2. The indices were measured for each standard star on 13 spectra obtained by subtracting the sky spectrum taken from different (not adjacent) slits. It is seen from this table that the standard deviation does not exceed a few percent and is larger for the Balmer lines, Hδ_A, Hγ_A, Hδ_F, Hγ_F, located near the edges of the spectra.

References

Albayrak B., Gulliver A. F., Adelman S. J., Aydin C., Kocer D., A&A, **400**, 1043 (2003)

Afanasiev V.L, Moiseev A.V., AstL, **31**, 216 (2005)

Brusual G., Charlot S., MNRAS, **344**, 1000 (2003)

Burstein,D., Faber S.M., Gaskell C.M., & Krumm N., ApJ, **287**, 586 (1984)

Chentsov E. L., Ermakov S. V., Klochkova V. G., Panchuk V. E., Bjorkman K. S., & Miroshnichenko A. S., A&A, **397**, 1035 (2003)

Geisler D., PASP, **100**, 687 (1988)

Faber S.M., ApJ, **179**, 731 (1973)

Puzia T.H., Saglia, R. P., Kissler-Patig, M. et al., A&A, bf 395, 45 (2002)

Rich R.M., AJ, **95**, 828 (1988)

Sharina M.E., Sil'chenko O.K., Burenkov A.N., A&A, **397**, 831 (2003)

Thomas D., Maraston C., Bender R., MNRAS, **339**, 897 (2003)

Tonry J., Davis M., AJ, **84**, 1511 (1979)

Rich R.M., AJ, **95**, 828 (1988)

Vazdekis A., ApJ, **513**, 224 (1999)

Worthey G. ApJS, **95**, 107 (1994)

Worthey G., Ottaviani D.L., ApJS, **111**, 377 (1997)

Worthey G., Faber S.M., Gonzalez J.J., Burstein D., ApJS, **94**, 687 (1994)